IEEE Photonics Journal
An IEEE Photonics Society Publication

Amplitude-Independent Photonic Instantaneous Frequency Measurement With Improved Sensitivity

Volume 4, Number 5, October 2012

Niusha Sarkhosh, Member, IEEE
Hossein Emami, Member, IEEE
Arnan Mitchell, Member, IEEE

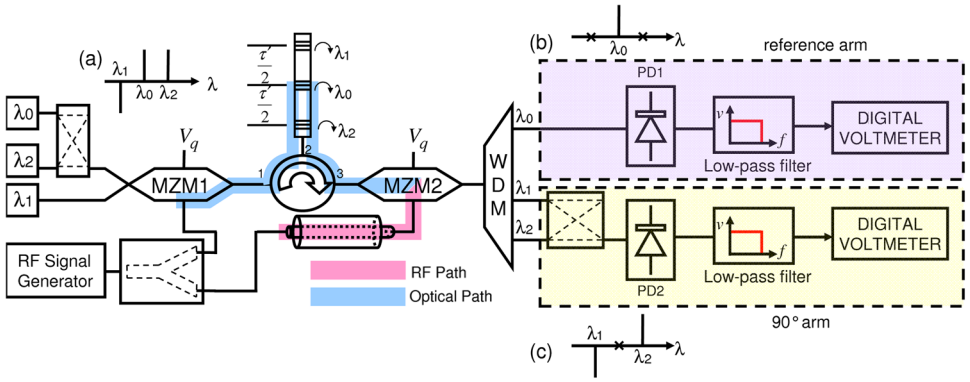

DOI: 10.1109/JPHOT.2012.2212005
1943-0655/$31.00 ©2012 IEEE

Amplitude-Independent Photonic Instantaneous Frequency Measurement With Improved Sensitivity

Niusha Sarkhosh,[1] *Member, IEEE*, Hossein Emami,[2] *Member, IEEE*, and Arnan Mitchell,[3] *Member, IEEE*

[1]Department of Electrical Engineering, University of California, Los Angeles, CA 90024 USA
[2]Department of Electrical Engineering, Majlesi Branch, Islamic Azad University, Isfahan, 8631656451, Iran
[3]School of Electrical and Computer Engineering, RMIT University, Melbourne, VIC. 3001, Australia

DOI: 10.1109/JPHOT.2012.2212005
1943-0655/$31.00 ©2012 IEEE

Manuscript received June 2, 2012; revised July 28, 2012; accepted August 1, 2012. Date of publication August 7, 2012; date of current version August 17, 2012. Corresponding author: N. Sarkhosh (e-mail: niusha@ucla.edu).

Abstract: A technique for improving the sensitivity of a class of broadband RF photonic instantaneous frequency measurement (IFM) systems is proposed and practically demonstrated. The technique utilizes lock-in amplification to isolate the desired signal from background noise. The demonstration is conducted on a dual orthogonal measurement IFM system utilizing multiple wavelengths and a transversal Hilbert transform achieving independent amplitude and frequency measurements over a multioctave bandwidth with a sensitivity of −37 dBm. This performance is comparable with traditional electronic IFM receivers. The successful application of this lock-in approach to this multichannel photonic system illustrates its flexibility and indicates that it should be applicable to even more sophisticated systems.

Index Terms: Microwave photonics, microwave photonics signal processing.

1. Introduction

Radar warning receivers are designed to detect and classify potential threats in an electronic warfare environment. RF signal processing techniques are exceptionally incisive; however, they can require some advance knowledge of the threat and can also require significant computation resources and time for processing. Instantaneous frequency measurement (IFM) systems have been developed as a means of obtaining a rapid indication of the presence of a potential threat and roughly identify the frequency of the threat signals, suggesting the frequency range in which to focus more sophisticated signal acquisition and processing resources.

Traditional IFM receivers have been deployed for many years [1]. Systems can provide good frequency measurement range (.5–18 GHz) with sensitivity of −50 dBm [2]. In recent years, electronic warfare systems operating in the millimeter-wave regime (.5–40 GHz) have become desirable. It is difficult to realize traditional microwave implementations that can provide such broad bandwidth operation [3], [4].

Microwave photonics (MWP) has been introduced [5]–[7] as a means of broadband signal processing, providing immunity to electromagnetic interference and eliminating the need for broadband impedance matching networks. Therefore, it would be advantageous to utilize MWP to implement a broadband IFM system. Several photonic IFM systems have been reported.

A frequency measurement concept has been demonstrated based on the amplitude comparison of power fading functions generated by double sideband modulated optical carriers propagating through a dispersive medium [8]. A similar power fading approach has been demonstrated in [9] where phase modulation and polarization diversity are utilized to eliminate one laser. A novel IFM receiver based on optical signal remodulation was proposed in [10]. Both RF power and frequency were measured using a modulation–remodulation scheme and a resolution of 3 MHz over a frequency range of 12 GHz was achieved A microwave frequency measurement technique flexible in terms of frequency range and resolution based on stimulated Brillouin scattering, was reported in [11]. The technique provided either wide frequency measurement range of 12 GHz with $\pm$250 MHz resolution or narrow measurement range of 2 GHz with higher resolution of $\pm$50 MHz.

We have reported a photonic IFM system based on down-converting high-frequency RF signals to dc in the optical domain allowing detection using low-frequency photodetectors (PDs) [12]–[14]. The demonstrated system provides a frequency measurement bandwidths comparable with the traditional IFM receivers, with the added flexibility offered by photonic systems. However, the sensitivity of this system remained in question.

We have quantified the sensitivity of the proof of concept system of [12] and demonstrated that lock-in amplification can be used to significantly improve the sensitivity without compromising RF bandwidth [15]. This demonstration implemented only a single IFM and was thus unable to independently measure the RF frequency and amplitude.

In this paper, we present a significant extension of [15] by refining our lock-in amplification approach and demonstrating that it can be applied to two orthogonal photonic IFM systems in parallel and, further, that it is compatible with our multiwavelength photonic transversal Hilbert transform [16]. The result is a significant advancement of the dual orthogonal system reported in [13], which is capable of measuring both RF frequency and power simultaneously and independently with a sensitivity of $-$37 dBm over 10-GHz frequency range. This demonstration proves that our relatively simple sensitivity enhancement approach can be applied to a sophisticated parallel photonic IFM architecture to provide comparable sensitivity to traditional electronic systems while maintaining the exceptional flexibility and bandwidth that are characteristic of photonic systems.

The paper is organized as follows: Section 2 presents a review of the photonic IFM system demonstration of [13] and then extends the analysis to quantify the system sensitivity. Section 3 presents a theoretical analysis of the dominant sources of noise and interference that limit the sensitivity and predicts the improvement that should be achievable through the use of lock-in amplification. Sections 4 and 5 then present a demonstration of an improved photonic IFM system incorporating lock-in amplification and demonstrates that the sensitivity achieved is close to the theoretical limit.

2. Parallel Orthogonal Photonic IFM

We have already demonstrated a low-cost microwave photonic IFM system capable of measuring both RF frequency and power simultaneously and independently [13]. This previous report did not investigate the system sensitivity. This section reviews this IFM system and then quantifies the system sensitivity and discusses potential limitations on this sensitivity.

2.1. Photonic IFM System

Fig. 1 shows the experimental setup of the photonic IFM system with orthogonal outputs. An RF signal generator produced a single RF tone with angular frequency of Ω, which was divided into two equal portions feeding two arms of the IFM system. These arms are labeled the "optical path" and the "RF path" in Fig. 1. The RF tone in the optical path modulated three wavelengths being used to implement a two-tap (λ_1 and λ_2) transversal filter with a reference tap $(\lambda_\circ)$ in between. Carriers $\lambda_\circ$ and λ_2 were combined using a 3-dB optical coupler. This combined signal, together with λ_1, was modulated oppositely by MZM 1 to make the desired combination, as shown in the inset in Fig. 1(a) [13]. The modulated signal was then input to port 1 of an optical circulator. Port 2 of the circulator was connected to a cascaded grating where each wavelength was reflected with different but

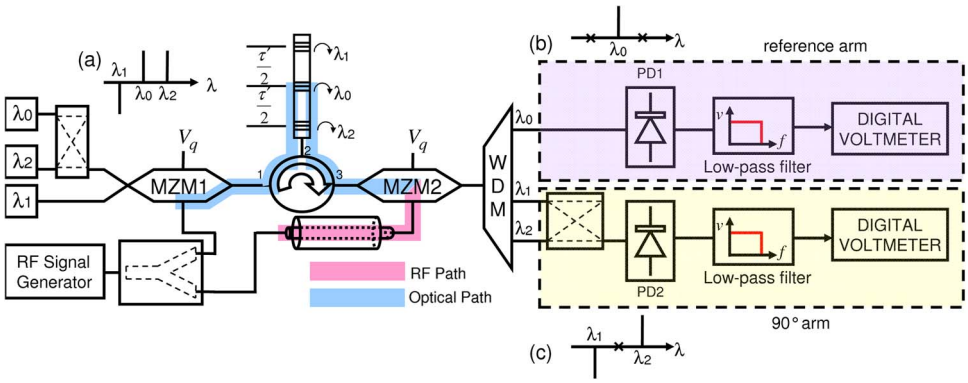

Fig. 1. Experimental setup of the original IFM system.

uniformly incremented delays. The dispersed signal was output from port 3 and input to MZM 2 fed with the original RF tone traversed through a coaxial cable in the RF path. To ensure correct polarization at the MZM 2 input, both cascaded grating and optical circulator were selected to be polarization maintaining (PM). The output of MZM 2 was then input to a wavelength division multiplexer (WDM), which separates all wavelengths. Carrier $\lambda_\circ$ remained separated and was used as the reference [see inset in Fig. 1(b)]. The arm containing $\lambda_\circ$ was called the reference arm. Carriers λ_1 and λ_2 were again combined using a 3-dB coupler to make the two-tap transversal filter [see inset in Fig. 1(c)]. This arm was called the 90° arm. Both signals were then detected by low-frequency PDs (PD1 and PD2), low-pass filtered, and measured by digital voltmeters.

It can be shown that the output voltages of the reference arm $(V_\circ)$ and the 90° arm (V_{90}) can be expressed as

$$V_{\mathrm{DC}_\circ}(\Omega) \approx \frac{1}{4} G Z_{\mathrm{PD}} P_\circ \left[1 + \frac{\pi^2(1+M^2) Z_{\mathrm{in}} P_{\mathrm{RF}}}{4V_\pi^2}\right] + \frac{\pi^2}{4V_\pi^2} GMZ_{\mathrm{PD}} Z_{\mathrm{in}} P_\circ P_{\mathrm{RF}} \cos\phi \tag{1}$$

$$V_{\mathrm{DC}_{90}}(\Omega) \approx \frac{1}{2} G Z_{\mathrm{PD}} P_{90} \left[1 + \frac{\pi^2(1+M^2) Z_{\mathrm{in}} P_{\mathrm{RF}}}{4V_\pi^2}\right] + \frac{\pi^2}{2V_\pi^2} GMZ_{\mathrm{PD}} Z_{\mathrm{in}} P_{90} P_{\mathrm{RF}} \sin\frac{\Omega\tau'}{2} \sin\phi \tag{2}$$

where Z_{in} and Z_{PD} are the input impedance of the MZMs and output impedance of the PDs, respectively. V_π is the half-wave voltage of MZMs. $P_\circ$ is the optical power of carrier $\lambda_\circ$ present at the input of the MZM 1, and P_{90} is the optical power of carriers λ_1 and λ_2 present at the input of MZM 1, which should be equal. P_{RF} is the RF power present at the input of the Wilkinson power divider. τ' is the delay between λ_1 and λ_2 caused inside the cascaded grating. M is the absolute magnitude response of the RF path, which could be function of frequency as the RF path may have frequency-dependent loss. ϕ is the phase response of the RF path relative to the optical path. In case of having no dispersion, $\phi = \Omega\tau$ where τ is the delay between the RF and optical paths. The factor G is defined as

$$G = rG_{\mathrm{LPF}} L_{\mathrm{MZM}}^2 L_{\mathrm{WDM}} \tag{3}$$

where r is the responsivity of the PD, and G_{LPF}, L_{MZM}, and L_{WDM} are the gain values of the low-pass filter, the MZM optical insertion loss, and WDM optical insertion loss, respectively. Note that it is assumed that the MZMs and PDs are identical. Using (1) and (2), P_{RF} and Ω can thus be identified independently. Having conceived a photonic IFM system capable of measuring the RF frequency with unknown power level, it is now possible to analyze the sensitivity of the system.

3. Sensitivity Analysis

This section aims to predict theoretically the noise floor of the IFM system of Section 2.1. In an optical link, the total noise of the system can be described as a summation of shot noise, RIN noise,

and thermal noise

$$\overline{n} = \overline{n_{\text{shot}}} + \overline{n_{\text{RIN}}} + \overline{n_{\text{Th}}}. \tag{4}$$

Shot noise can be described as

$$\overline{n_{\text{shot}}} = 2qI_D BZ_\circ \tag{5}$$

where q is the charge of a single electron, I_D is the bias current of the PD, B is the bandwidth of the system, and $Z_\circ$ is the load impedance. The RIN noise can be describe as

$$\overline{n_{\text{RIN}}} = I_D^2 \text{RIN}_{\text{laser}} BZ_\circ \tag{6}$$

where $\text{RIN}_{\text{laser}}$ is the relative intensity of the laser. The thermal noise can be written as

$$\overline{n_{\text{Th}}} = kT_\circ B \tag{7}$$

where k is the Boltzmann constant and T is the operating temperature in kelvins. In the system of Section 2.1, the optical power was of the order of 10 dBm, and thus, the PD current (I_D) was on the order of 10 mA. The shot noise will thus be far greater than the thermal noise. The laser RIN of our DFB lasers was specified at -145 dB/Hz. Thus, using (5) and (6), it is possible to estimate the noise floor of the system that could be obtained through the use of lock-in amplification. Although the lock-in amplifier can be set with a bandwidth of kHz or even Hz, the actual noise bandwidth sampled by the system will be limited by the linewidth of the optical carrier. The linewidth of our DFB laser was 1 MHz. Thus, having an optical power of 10 mW and $Z_\circ = 50\ \Omega$, leading to an approximate detector current of $I_D = 10$ mA (assuming ideal responsivity), we can use (5) and (6) to calculate the noise in the optical signal as $\overline{n_{\text{shot}}} = -64$ dBm, and $\overline{n_{\text{RIN}}} = -54$ dBm. Thus, the minimum detectable RF signal is

$$\overline{n} = \overline{n_{\text{shot}}} + \overline{n_{\text{RIN}}} = 2qI_D BZ_\circ + I_D^2 \text{RIN}_{\text{laser}} BZ_\circ. \tag{8}$$

Therefore, the minimum detectable RF signal was calculated to be -53.8 dBm. Having analyzed the sensitivity of the IFM system, it must be confirmed practically.

3.1. Sensitivity Measurement

The system was setup as shown in Fig. 1. The optical carriers were set to $\lambda_\circ = 1550$, $\lambda_1 = 1551.5$, and $\lambda_2 = 1548.5$ nm. The optical powers corresponding to these three wavelengths were set to 16, 11.7, and 15.8 mW, respectively. This resulted in $P_\circ = 11.7$ and $P_{90} = 12$ mW. The half-wave voltage of MZMs was $V_\pi = 5$ v and $\tau' = 80$ ps. The factor G was calculated to be 0.95. Since wavelengths of optical carriers were selected very close to each other, V_π was the same for all optical carriers. During the experiment, it was ensured that both MZMs remained biased at quadrature point (V_q). This was done by manually adjusting the bias points after each measurement.

Fig. 2(a) shows the frequency response of the IFM system with input RF powers of 7, 1, and -2 dBm. Note that continuous lines show the prediction results from 1 and 2, while squares and triangles show the measured results. We have called the output of the reference arm "cos" since, as described by 1, it should exhibit a cosine shape. The output of 90° arm was called "sin" since, as described by 2, it should exhibit a sinuous shape.

In Fig. 2(a) at the RF power of $P_{\text{RF}} = 7$ dBm, the sinusoidal transfer function is clearly evident, and the amplitude of the variations is a significant proportion of the observed dc offset. At $P_{\text{RF}} = 1$ dBm, the sinusoidal response is still observable, but the amplitude is significantly reduced. Conversely, the frequency-invariant dc offset remains almost unchanged with the reduced RF input power. Reducing the RF power to $P_{\text{RF}} = -1$ dBm resulted in attenuation of the amplitude of the sinusoidal transfer function to the scale of the noise on the dc offset. As it can be seen, the sensitivity of the IFM system in Fig. 1 is not below -2 dBm.

To better illustrate the noise floor behavior, the amplitude difference of the output was measured as a function of the input RF power. The output signal amplitude difference was defined as the

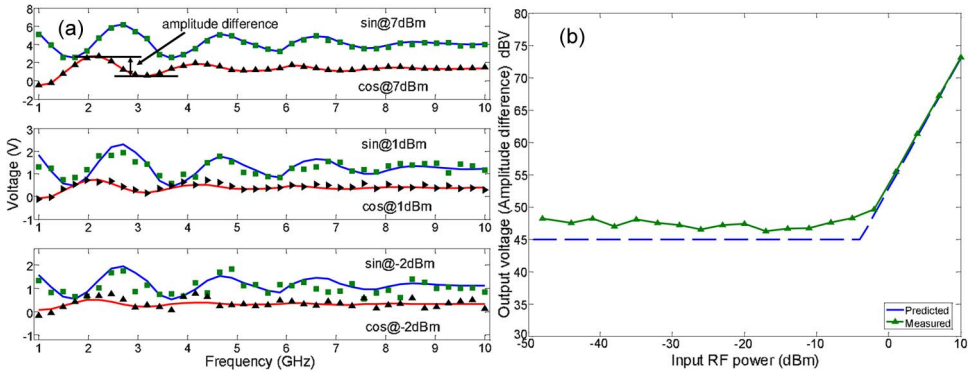

Fig. 2. (a) Output voltage of IFM system as a function of frequency at 7-, 1-, and −2-dBm RF input power. (b) Amplitude difference of the output for different RF input powers.

voltage difference between the first peak and the first null in the oscillating response, as illustrated in Fig. 2(a). Measurements were taken for input RF powers ranging from 10 to −50 dBm in 3-dB decrements. Fig. 2(b) shows the amplitude of the output as a function of the RF input power for the original system in Fig. 1. A sensitivity of only −2 dBm was achieved. At this power, it is no longer possible to measure frequency with this system. Recall that the role of an IFM system in a RADAR warning receiver is to provide early indication of possible threats in an electronic warfare environment. The ability to see distant threats is vital, and hence, the sensitivity of an IFM system is extremely important.

It has been established that the sensitivity of the experiment in Fig. 1 is between −2 dBm and 1 dBm. This poor level of sensitivity would be unacceptable in practical applications. It is thus necessary to explore methods for enhancing the sensitivity of this IFM system if it is to be seriously considered for RADAR warning receiver applications. The poor sensitivity observed in Fig. 2(a) can be attributed to the fact that measurements have been conducted at dc and with practically no filtering. There are numerous sources of electrical noise close to dc; the most significant of these is current noise. The traditional method for removing noise sources close to dc is to use lock-in amplification.

4. Sensitivity-Enhanced Photonic IFM

The poor sensitivity shown in Section 2 has been attributed to the strong frequency-invariant dc component predicted by (1) and (2), which quickly dominates the output response as the input RF signal amplitude is reduced. If this frequency-invariant component could be rejected by the receiver, then a far more sensitive measurement should result.

The signal processing technique of lock-in amplification may be able to help. A lock-in amplifier perturbs the measurement system with a dithering tone and then, on detection, mixes the received signal with the same dithering tone to extract the desired measurement and eliminate background noise. To be effective, it is important that the perturbation modifies the components of the output that are of interest while leaving the background interference unchanged [17].

For the IFM system in Fig. 1, the quantity we are trying to measure is the RF frequency, and we are doing this by relating the phase (ϕ) accumulated by a fixed delay (τ) to the signal frequency. Thus, to effectively use lock-in amplification, this differential time difference must be modulated with a dithering tone. Equations (1) and (2) show that perturbing τ will only change the desired frequency-dependent component of the output, leaving the frequency-independent components unaltered. Having established that it is the time delay (τ) that must be modulated, it is now necessary to conceive a system that will enable modulation of this delay with sufficient amplitude and frequency to enable lock-in amplification.

In order to achieve lock-in amplification, the delay τ must be modulated at a rate of a few hundred Hz and with sufficient amplitude that the phase change imparted by the varying delay can be

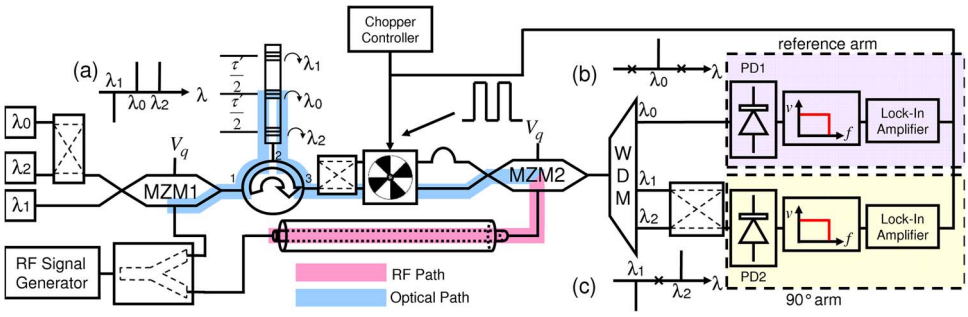

Fig. 3. Experimental setup of the sensitivity enhanced IFM system.

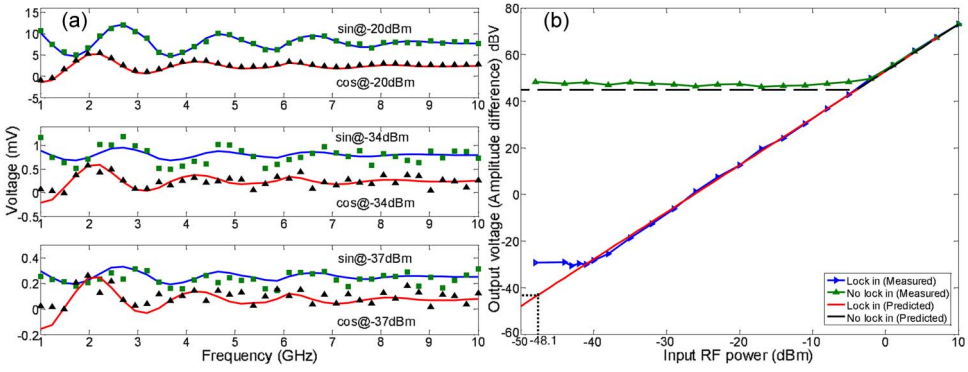

Fig. 4. a) Output voltage of IFM system as a function of frequency at −20-, −34-, and −37-dBm RF input power. b) Amplitude difference of the output for different RF input powers.

observed interferometrically. This means that the physical change in path length must be of the order of 1% of a wavelength at the lowest frequency to be measured. In the case of the system of Section 2, the minimum frequency is 1 GHz, and so, the physical change in length must be a significant fraction of a centimeter. One might consider electro- or thermooptic phase modulation or even fiber stretching as a means of perturbing the path length; however, these approaches will be insufficient to achieve the large changes in delay required for this investigation. We have chosen instead to use a physical switching between two paths to achieve the required modulation.

Fig. 3 shows the experimental setup of the sensitivity-improved IFM receiver with orthogonal measurement. The setup is similar to the setup in Fig. 1 until port 3 of the circulator. After this, the optical signal was input to a PM 3-dB optical splitter. The outputs of the splitter were input to the space with different optical path lengths, and the mechanical chopper was inserted in the path of both beams. After passing through the chopper, the free space optical signals were collected, and both refocused into separate PM optical fibers. The signals were connected to a 2×1 MZM (MZM 2) fed with the original RF tone in the RF path. The output of MZM 2 then fed both reference and 90° arms via the WDM. This time, however, both signals were measured by lock-in amplifiers, which had a reference from the dithering signal controlling the chopper.

Having conceived an improved sensitivity photonic IFM system capable of producing orthogonal measurement, it is now possible to demonstrate the sensitivity improvement of the system.

The system was configured as depicted in Fig. 3 with the same specifications as before. The bandwidth of the lock-in amplifier was chosen to be 1 kHz.

Then response of the system of Fig. 3 was measured for the input RF powers of −20 dBm, −34 dBm, and −37 dBm. Fig. 4(a) shows the IFM response for different RF powers. Compared with Fig. 2(a), it is clear that the sensitivity has improved dramatically. The amplitude of frequency-varying component of the response still dominates even at −20-dBm input power. Reducing the

input power to −34 dBm, it is still possible to observe the frequency-varying response. At −37 dBm, the response has been lost in the noise floor of the system. It is worth noting that the response still maintains a frequency-invariant dc offset, which appears to be proportional to RF input power. This is as expected from (1) and (2).

To further illustrate the noise floor performance, the amplitude of the output was measured as a function of the input RF power. Sequential measurements of the frequency response were taken with incrementally diminishing input RF powers starting from 10 dBm to −50 dBm in 3-dB decrements.

Fig. 4(b) shows the amplitude difference of the output as a function of the RF input power for the original system in Fig. 1 and the improved sensitivity system in Fig. 3 using the chopper as the optical switch. From Fig. 4(b), it is clear that the system without lock-in amplification can only achieve sensitivity of −2 dBm, while the locked system can achieve sensitivity of −37 dBm. This confirms the observations in Figs. 2(a) and 4(a). This sensitivity, however, is still far from the predicted value of −79 dBm. In the next section, we will further investigate this issue.

5. DC Offset Due to Insertion Loss Difference in Chopper Arms

As shown in Fig. 3, the chopper alternates the light way between two paths. In practice, these paths have different insertion losses. This difference can result in a dc offset in lock-in measurement, as can be seen in Fig. 4(a). This dc offset may result in less sensitivity. To predict the sensitivity degradation due to this issue, consider 1. This equation has a frequency-independent part as below

$$V(P_\circ) = \frac{1}{4} G Z_{\mathrm{PD}} P_\circ. \tag{9}$$

Since two arms of the chopper exhibits different losses, the optical power at the input of PD would be different for each path, and thus, at the lock-in output, there will be a dc offset of

$$V_{\mathrm{OFFSET}} = \frac{1}{4} G \Delta L Z_{\mathrm{PD}} P_\circ \tag{10}$$

where ΔL is the difference between insertion losses of the chopper arms. This coefficient is responsible for optical power changes in the system. We measured ΔL as 0.0372. Therefore, the predicted dc offset can be calculated as −42.67 dBV. From Fig. 4(b), the predicted sensitivity can be found as −48.1 dBm, which is almost 11 dB less that the measured sensitivity of −37 dBm. This could be caused by instabilities occurred in a discrete photonic system specifically due to polarization mismatch occurred at fiber pigtail connections. Integrating the system could result in better sensitivity. Electrooptic switches could then be employed instead of the mechanical chopper. This would make the system more practical to be employed in a RADAR warning receiver, which is supposed to work in the harsh battle environment. It is conceivable that this technique could be applied to an all-optical mixing IFM system [14] to achieve even broader bandwidth.

6. Conclusion

The sensitivity of a photonic IFM receiver capable of producing orthogonal measurements has been improved using lock-in amplification scheme, and a sensitivity of −37 dBm was achieved. This was done based on a dithering technique where the actual optical lengths were employed along with an optical chopper as a switch to achieve different delays.

References

[1] J. B. Y. Tsui, "Instantaneous frequency measurement receiver with digital processing," U.S. Patent 4 633 516, Dec. 30, 1986.

[2] *Wide Band Systems, Instantaneous Frequency Measurement Receiver Systems (IFM)*, Wide Band Systems, Inc., Rockaway, NJ. [Online]. Available: http://www.widebandsystems.com/ifm.html

[3] S. Kumar, A. Mohammadi, and D. Klymyshyn, "A direct 64QAM modulator suitable for MMIC applications," *Microw. J.*, vol. 40, no. 4, pp. 116–122, Apr. 1997.

[4] Y. Zhu, "A 10–40 GHz 7 dB directional coupler in digital CMOS technology," in *Proc. IEEE MTT-S Int. Microw. Symp. Dig.*, Jun. 2006, pp. 1551–1554.
[5] J. Capmany and D. Novak, "Microwave photonics combine two worlds," *Nat. Photon.*, vol. 1, no. 6, pp. 319–330, Jun. 2007.
[6] R. A. Minasian, "Photonic signal processing of microwave signals," *IEEE Trans. Microw. Theory Tech.*, vol. 54, no. 2, pp. 832–846, Feb. 2006.
[7] A. J. Seeds and K. J. Williams, "Microwave photonics," *J. Lightw. Technol.*, vol. 24, no. 12, pp. 4628–4641, Dec. 2006.
[8] L. V. T. Nguyen and D. B. Hunter, "A photonic technique for microwave frequency measurement," *IEEE Photon. Technol. Lett.*, vol. 18, no. 10, pp. 1188–1190, May 2006.
[9] J. Zhou, S. Fu, P. P. Shum, S. Aditya, L. Xia, J. Li, X. Sun, and K. Xu, "Photonic measurement of microwave frequency based on phase modulation," *Opt. Exp.*, vol. 17, no. 9, pp. 7217–7221, Apr. 2009.
[10] M. V. Drummond, C. A. F. Marques, P. P. Monteiro, and R. N. Nogueira, "Photonic instantaneous microwave frequency measurement system based on signal remodulation," *IEEE Photon. Technol. Lett.*, vol. 22, no. 16, pp. 1226–1228, Aug. 2010.
[11] W. Li, N. H. Zhu, and L. X. Wang, "Brillouin-assisted microwave frequency measurement with adjustable measurement range and resolution," *Opt. Lett.*, vol. 37, no. 2, pp. 166–168, Jan. 2012.
[12] N. Sarkhosh, H. Emami, L. A. Bui, and A. Mitchell, "Reduced cost photonic instantaneous frequency measurement system," *IEEE Photon. Technol. Lett.*, vol. 20, no. 18, pp. 1521–1523, Sep. 2008.
[13] H. Emami, N. Sarkhosh, L. A. Bui, and A. Mitchell, "Amplitude independent RF instantaneous frequency measurement system using photonic Hilbert transform," *Opt. Exp.*, vol. 16, no. 18, pp. 13707–13712, Sep. 2008.
[14] N. Sarkhosh, H. Emami, L. Bui, and A. Mitchell, "Photonic instantaneous frequency measurement using non-linear optical mixing," in *Proc. IEEE MTT-S Int. Microw. Symp. Dig.*, Jun. 2008, pp. 599–601.
[15] N. Sarkhosh, H. Emami, L. Bui, and A. Mitchell, "Microwave photonic instantaneous frequency measurement with improved sensitivity," in *Proc. IEEE MTT-S Int. Microw. Symp. Dig.*, Jun. 2009, pp. 165–168.
[16] H. Emami, N. Sarkhosh, L. A. Bui, and A. Mitchell, "Wideband RF photonic in-phase and quadrature-phase generation," *Opt. Lett.*, vol. 33, no. 2, pp. 98–100, Jan. 2008.
[17] D. Green, "Lock-in, tracking, and acquisition of AGC-aided phaselocked loops," *IEEE Trans. Circuits Syst.*, vol. 32, no. 6, pp. 559–568, Jun. 1985.